JOURNAL OF THE KOREAN ASTRONOMICAL SOCIETY
29: 245~253, 1996

AN ANALYSIS OF INFRARED IMAGES OF JUPITER IMPACTED BY P/SHOEMAKER-LEVY 9 *

KIM, YONG HA AND SUNG, KIYUN
Department of Astronomy and Space Science, Chungnam National University
KIM, SANG JOON
Kyunghee Observatory, Institute of Natural Sciences,
Department of Astronomy and Space Science, Kyunghee University
W. D. COCHRAN, D. F. LESTER, L. TRAFTON, AND B. E. CLARK
Department of Astronomy, University of Texas, Austin, U.S.A
(Received September 20, 1996; Accepted October 11, 1996)

ABSTRACT

We have analyzed infrared (IR) images of Jupiter which was observed at the McDonald Observatory, Texas, U.S.A., during the P/SHoemaker-LEvy 9 (SL9) impact period and about one week after the last impact. The IR images were obtained on the 2.7m telescope using a NICMOS array with filters to isolate the 1.5 μm NH_3 band, the 2.3 μm CH_4 band, the 2.12 μm H_2 S(0) pressure-induced absorption, and the continua at 1.58 μm and 2.0 μm (short K-band). All images except those with the 1.58 μm continuum filter show bright impact sites against the relatively dark Jovian disk near the impact latitude of about 45° S. This implies that dusts originated from the impacts reflect the solar radiation at high altitudes before absorbed by stratospheric CH_4, NH_3 or H_2. The impact sites observed with the 2.3 μm filter are conspicuously bright against a very dark background. The morphology of impact sites, G, L, and H at 2.3 and 2.12 μm filters shows clearly an asymmetric structure toward the incident direction of the comet fragments, in agreement with the studies of visible impact images obtained with the Hubble Space Telescope. Comparisons of reflectances of G, L, and H sites with simple radiative transfer models suggest that optically thick dust layers were formed at high altitudes at which methane absorption attenuates incoming sunlight only by about 1 %. The dust layers in these sites seem to form at about the same altitude regardless of the magnitude of the impacts, but they appear to descend gradually after the impacts. The dust layers have optical depths of 2 - 5, according to the models.

Key Words : Planet:Jupiter, Comet:impact, Infrared:imaging

I. INTRODUCTION

It has been heralded in mass media that fragments of the comet Shoemaker-Levy 9 (SL9) impacted on Jupiter during a period of July 16 - 22, 1994. The SL9 was discovered by Shoemaker and Levy as a series of fragments in March, 1993 and soon predicted to collide with Jupiter by Nakano and Marsden (see Time magazine page 42, May 23, 1994). Subsequent observations revealed about 21 fragments, some of which were divided into more fragments or faded away on their way to Jupiter (Weaver et al, 1995). As the fragments entered the Jupiter's atmosphere with a speed of 60 km/s, severe friction by atmospheric gas caused their explosions above or near the ammonia cloud level of Jupiter, showing more prominent fireballs and plumes than most predicted models (Sekanina, 1993; Zahnle and MacLow, 1994).

All the fragments were impacted at jovicentric latitudes of 43 - 45°S and just beyond the morning terminator (Hammel, et al, 1995). The exact locations of impacts were less than a degree away from predicted locations by

* This research was supported by a grant from the Korea Astronomy Observatory

Table 1. IR Observations of comet Shoemaker-Levy 9's collision with Jupiter

Begin Time (UT)	End Time (UT)	Begin CML	End CML	Impact sites
July 18 00:10	July 18 04:04	14.6	160	A(3) B(2) C(2) D(1) E(1)
July 19 00:05	July 19 06:20	159	17	A(5) B(5) C(5) D(3) E(3) F(2) G(2) H(0)
July 20 00:00	July 20 06:00	309	167	A(8) B(7) C(7) D(6) E(6) F(5) G(4) H(3) K(1) L(0)
July 21 04:10	July 21 06:00	245	317	C(9) D(9) G(7) K(4) L(3) P2(1) Q2(1) R(0)
July 21 21:30	July 22 06:00	160	108	A(13) B(12) C(2) D(11) E(11) F(0) G(9) H(8) K(6) L(5) P2(3) Q2(3) R(2) S(1) T(0)
July 23 00:00	July 23 06:00	41	258	W(2) V(2) U(3) T(3) S(3) R(4) Q2(5) P2(6) N(6) L(7) K(9) H(10) G(11) F(12) E(13) D(13) C(14) K(14)
July 30 02:30	July 30 05:30	104	177	Most sites still seen
July 31 00:52	July 31 05:44	195	17	Most sites still seen
July 31 21:41	August 1 04:53	230	131	Most sites still seen

The number in parentheses is the number of rotations since the impact.

Chodas and Yoemans (private communications, 1994). The exact impact moments could not be seen from earth, but rising and expanding fireballs subsequent to explosion were successfully observed by Hubble Space Telescope (HST) and ground-based telescopes (Hammel et al, 1995; references in Orton et al, 1995). The impact sites were observed to be bright in infrared, but dark brown in visible wavelengths for several months after the impacts. A substantial amount of dusts were produced from an expanding fireball and subsequently formed a layer of dusts in the upper atmosphere around each impact site (e.g. West et al, 1995). Characteristics of the impact dusts and dust layers are still being investigated in various observational and theoretical works .

Since the dust layer was formed in the upper atmosphere, and at methane (2.3 μm), H_2 (2.12 μm), ammonia (1.50 μm) absorption wavelengths sunlight can be reflected by a dust layer before absorbed in Jupiter's atmosphere, bright impact sites against dark backgrounds had been resulted. In the present work, we take this advantage to derive characteristics of the impact dust layers, namely, their altitudes and optical thicknesses from near infrared imaging observations.

II. OBSERVATIONS

Infrared imaging observations of Jupiter were carried out at the 2.7 m telescope of the McDonald observatory, operated by the University of Texas, Austin, during three periods: June 20 - 22 (prior to the comet impacts), July 16 - 22 (the comet impacting period), and July 29 - 31 (a week after the comet impact), 1994. The imaging detector used was a 256×256 HgCdTe CCD camera, manufactured by Rockwell, with a liquid nitrogen cooling system. The operating wavelength range of the CCD camera was between 1 and 2.5 μm. With an f/18 focal length ratio of the 2.7 m telescope, each pixel of the CCD camera subtends 0.4 arcsec of the celestial sphere. In order to detect sensitive effects on Jupiter's upper atmosphere by the comet impacts, we used four narrow band filters at 2.3 μm(CH_4 absorption band), 2.12 μm (H_2 collisionally induced absorption), 1.58 and 1.5 μm (NH_3 absorption wing and center, respectively). We have also used a semi-wide band filter at 2.0 μm that covers the short end of the standard K band.

More than 5 images of flat field for each filter were obtained by pointing at a white screen inside the dome every afternoon prior to observations. Average data count of 3000 per pixel was achieved within 1 - 20 seconds for the flat field images. Images of dark fields were also recorded every night to correct for any variation of detector noises. A sequence of observations consists of four image-takings toward sky, Jupiter, Jupiter, and sky in order. The sky image was taken from dark sky 180 arcsec away from Jupiter in the direction of declination with the same exposure time as one for the Jupiter's image. A sky-subtracted image of Jupiter was displayed on an observer's monitor

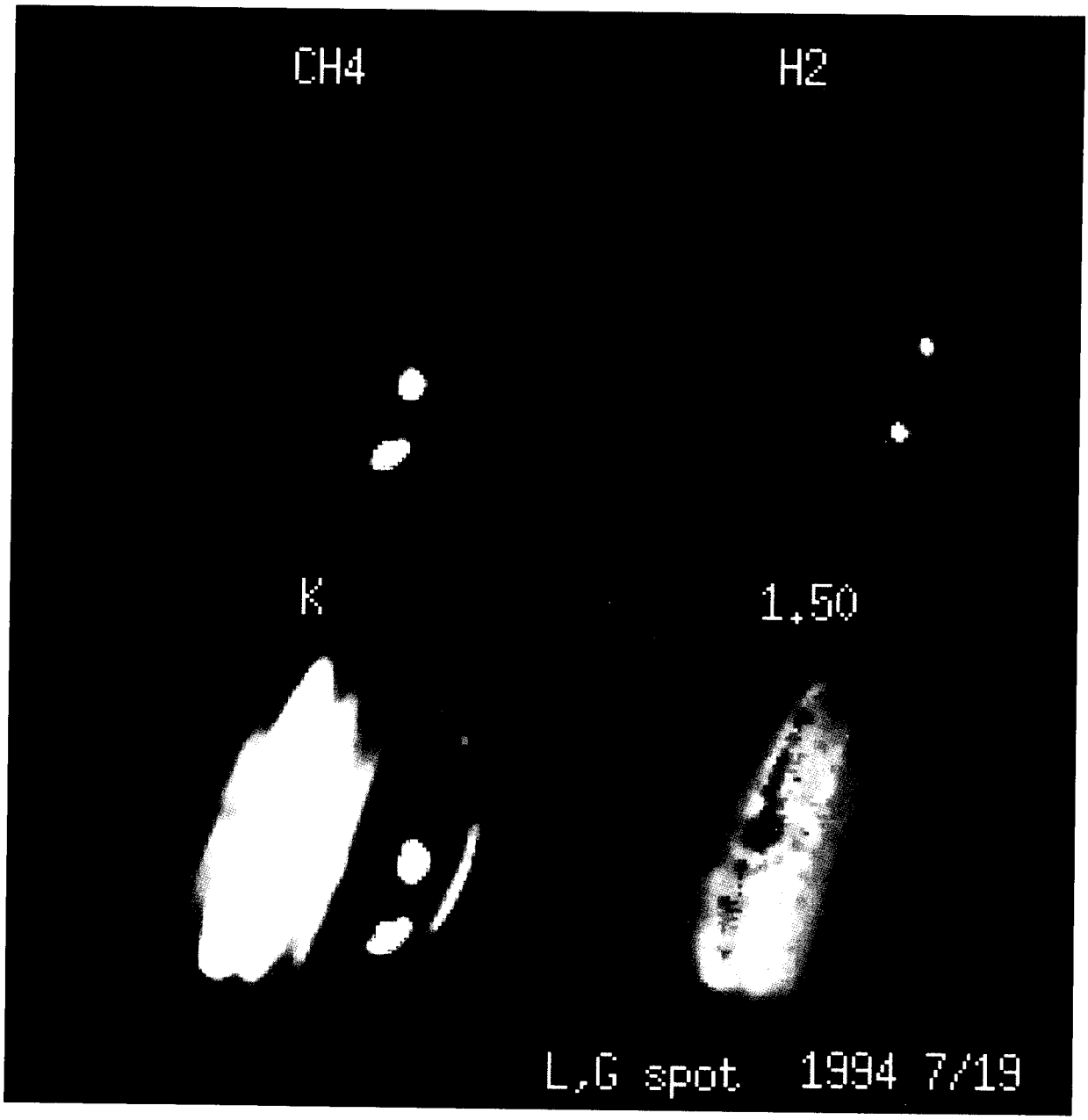

Fig. 1. Infrared images of Jupiter obtained with the CH_4 (2.3 μm), H_2 (2.12 μm), K (2 μm), and ammonia (1.50 μm) band filters. The impact sites of L, G, and H fragments are seen from lower to upper in series at a mid-latitude of the southern hemisphere.

immediately after one sequence of observations so that real-time decisions could be made on exposure times and the choice of filters.

The impact sites were best seen with the filters at CH_4 and H_2 absorption bands, since the disk of Jupiter is very dark due to the absorption at low altitudes and dusts from the impact at high altitudes reflect sunlight efficiently. Normally, exposure times of 10 to 20 seconds were used to obtain sufficient counts on each pixel with the CH_4 and H_2 filters. For the case of day-time observations during the impact of the U fragment on July 21, an exposure time of 0.5 second was used to reduce fast variations of bright daylight backgrounds. In order to record fast variation of brightness during the R impact, Jupiter's images were continuously taken with an exposure time as short as 2 seconds.

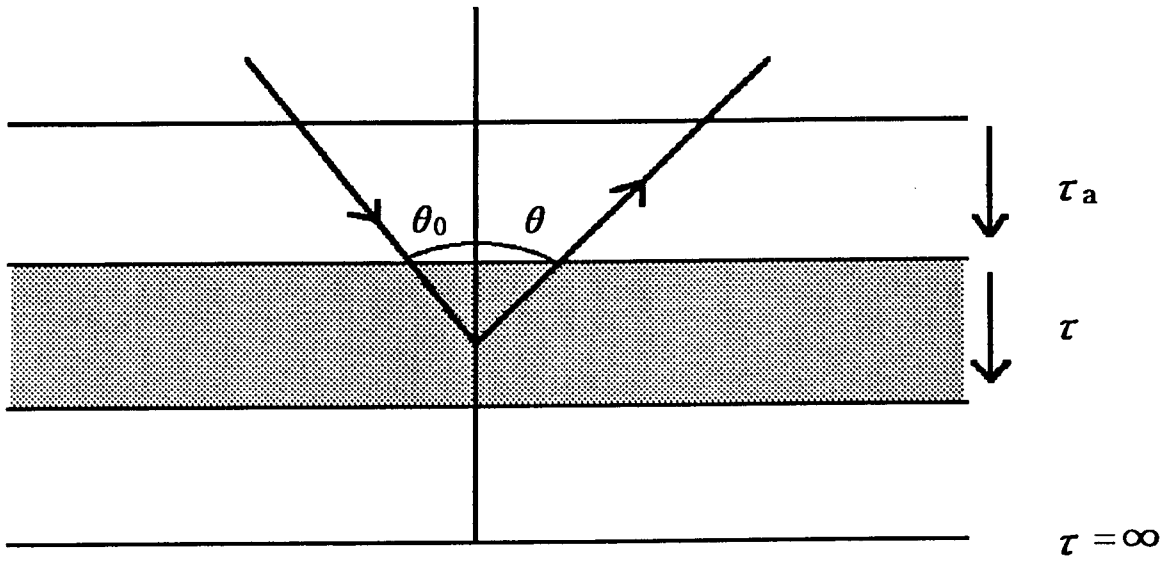

Fig. 2. A schematic diagram of a radiative transfer model for the impact dust layer.

During the observation period, the impact site of D fragment was first seen around 00:30 July 18 (hereafter time is in UT) and other impact sites were observed clearly in subsequent days. In particular, the impacts of F, R, U, V fragments were monitored with small time steps around the predicted impact times, but only the R impact was observed to have a clear brightness increase and decrease around the impact time. We present an analysis of the R impacting images in other paper (Kim and Kim, 1996). Table 1 shows the observing times, central meridians, and identities of impact sites seen during the observation periods.

The impact sites appear most clearly in CH_4 filter images, but their contrasts against the Jupiter disk diminish in H_2, short K, and 1.50 μm images, as shown in Figure 1. The impact sites of L, G, and H are seen from lower to upper in series at a mid-latitude of southern hemisphere in the CH_4 and short K filter images. The images were taken after the impact of L fragment on July 20. The H impact site is not seen in the H_2 and 1.50 μm images, which were taken prior to its appearing from the dawn limb. The images with the 1.58 μm filter do not show any trace of the impact. As we take the CH_4, H_2, short K, and 1.50 μm images in order, we effectively obtain appearances of Jupiter from high to low altitudes. Note that polar regions are bright in filters at longer than 2 μm since polar haze exists at high altitudes, unlike other regions.

III. MODEL

In order to derive the characteristics of impact dusts, we have developed a simple model in which a layer of dusts embedded in a semi-infinite atmosphere reflects incoming sunlight. This kind of model has been applied to haze particles in planetary atmospheres (West et al, 1995). As shown in figure 2, the model assumes the impact dust layer exists at an optical depth of τ_a due to atmospheric absorption. The dust layer itself has an optical depth of τ due to scattering of incident light by dust particles. Thus τ_a and τ represent altitude of the dust layer within the atmosphere and its thickness, respectively.

The intensity of outgoing light at the top of the dust layer may be expressed as

$$I_o(\mu) = \frac{\omega F}{4} \frac{\mu}{\mu + \mu_o} \frac{(1+\sqrt{3}\mu)(1+\sqrt{3}\mu_o)}{(1+k\mu)(1+k\mu_o)} (1 + P(\omega, \mu, \mu_o)) \quad (1)$$

(Chandrasekhar, 1960; Chamberlain and Hunten, 1987), with

$$P(\omega, \mu, \mu_o) = \frac{2k(\mu+\mu_o)(1-(1-\omega)^{1/2})e^{-2k\tau}}{(1-k\mu)(1-k\mu_o)(1+(1-\omega)^{1/2})} \quad (2)$$

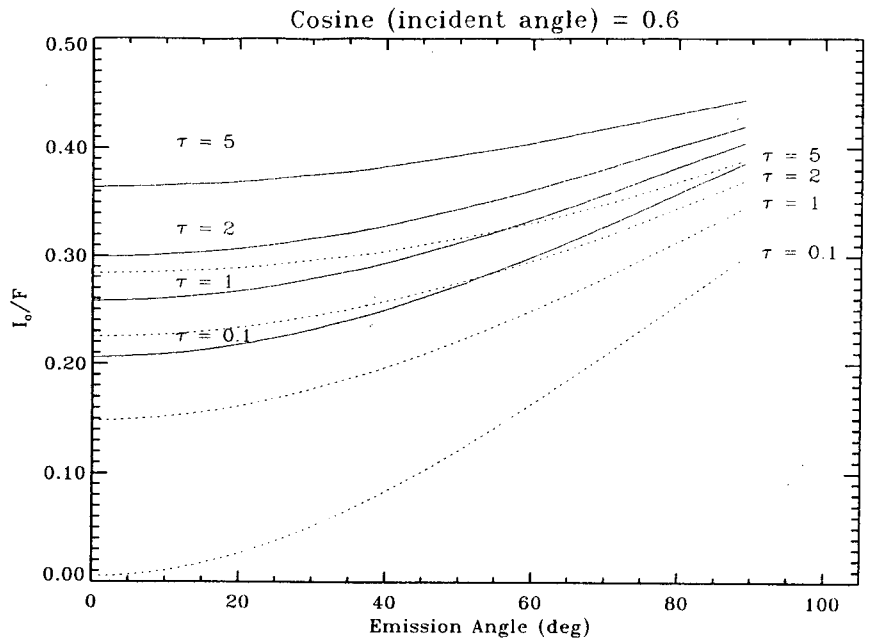

Fig. 3. Model reflectances of a dust layer with various optical depths as a function of emission angles for an incident angle of 53.1°.

$$k = (3(1-\omega))^{1/2}, \mu = cos\theta, \mu_o = cos\theta_o,$$

where ω is the single scattering albedo and πF is the solar flux at Jupiter's orbit. It is assumed that dust particles scatter light isotropically. The analytical expression of the outgoing intensity has been derived from an approximation based on two point Gaussian quadrature which may deviate from an exact solution by about 10% at worst (Chamberlain and Hunten, 1987). For the case of $\tau > 3$ and $\omega > 0.9$, an error of only a few percents results from the approximation. The assumptions and approximations are reasonable and widely used to estimate fundamental characteristics of a dust layer in the absence of detailed information on dust particles.

In figure 3 we show reflectances, I_o/F, of the dust layer as a function of emission angle for the cases of $\omega = 0.95$ and 0.99. Both cases assumes an incident angle of 53.1° ($\mu_o = 0.6$). The reflectance increases with emission angle, indicating that the dust layer is brighter in slant looking directions. For a given thickness of the layer, the reflectance increases with the single scattering albedo.

Since the atmosphere above the dust layer absorbs both incident and scattered light, the outgoing intensity at the top of Jupiter's atmosphere, which we observe from the earth, can be expressed as

$$I = I_o(\mu)exp(-\tau_a(1/\mu_o + 1/\mu)) \quad (3).$$

The cosine of an emission angle, μ, is 1 at the center of Jupiter's disk (sub-earth point), and close to 0 near the limb of visible disk, whereas the cosine of an incident angle, μ_o is 1 at the subsolar point and approaches to 0 at the terminator, the boundary of sun's illumination on Jupiter.

Since all the comet fragments fell on the latitude of about 45°S, we computed reflectance, I/F along the constant latitude line. The computed reflectances, I/F are presented as a function of distance from the central meridian longitude (CML) in figure 4. The negative numbers in the distance represent the morning side of Jupiter. The maxima of reflectances occur at a positive distance of about 2 arcsec because the subsolar point was at a longitude of 0.56° from CML in the afternoon side on July 15, 1994. Reflectance curves shown are for dust layer's optical depth, τ of 5, 2, 1, and 0.1 from the uppermost to the lowest one in the figure. For a dust layer thicker than $\tau = 5$, the reflectance curve is practically similar to one with $\tau = 5$. A higher single scattering albedo results in high reflectance, as expected. An average level of reflectances decreases with increasing optical depths of atmosphere above the dust layer, but increases with increasing optical depths of the dust layer. It is worth noting that the reflectance is reduced near CML for a dust layer thinner than $\tau = 1$, unlike those with thicker optical depths. This is because a thin dust layer becomes more transparent for light in nearly perpendicular direction than in slant directions.

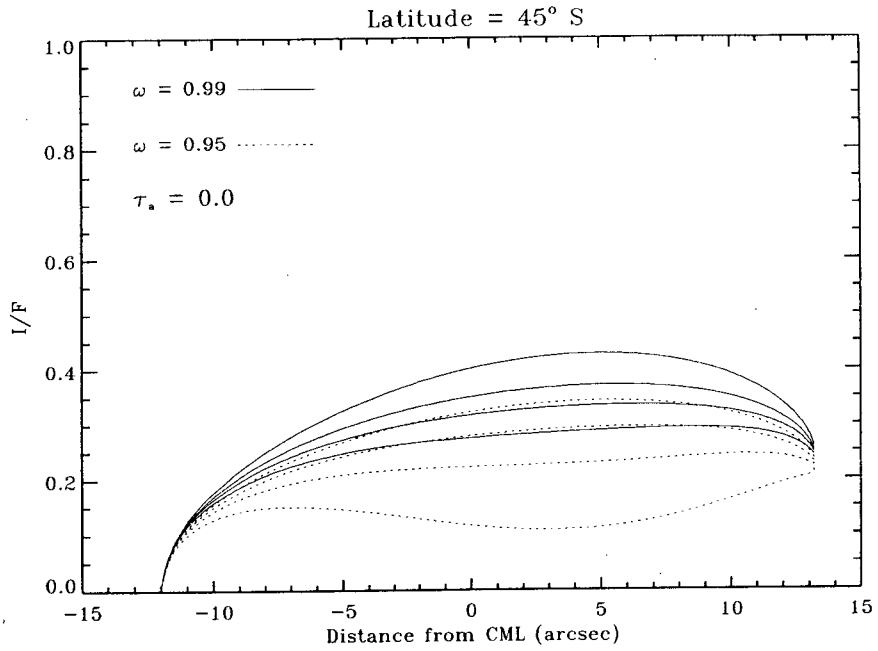

Fig. 4. Model reflectances of a dust layer with optical depths of 0.1, 2, and 5 (from lower to upper) as a function of anglular distance from the central meridian longitude of Jupiter. No atmospheric absorption above the dust layer was assumed.

IV. RESULTS AND DISCUSSION

In order to apply models to impact dust layers of impact sites, we converted relative intensities of impact sites into reflectances by assuming that polar haze's reflectance does not change over a period of days. The polar haze is bright in images taken with H_2 and CH_4 filters and is known to be stable within a timescale of weeks (Kim etal, 1991). The reflectances of polar haze were derived from comparison of its intensities with Io's intensities in the same frames, since Io's reflectance can be derived from a known geometric albedo, Λ_g of 0.77 at 2.3 μm (Clark and McCord, 1980; Nash et al, 1986). Io's reflectance may be expressed with a relation, $I/F = \Lambda_g \pi$. Derived reflectances of polar haze are $0.30\Lambda_g$ and $0.11\Lambda_g$ for H_2 and CH_4 filters, respectively.

For comparisons with models, we have chosen G and L images taken with the CH_4 and H_2 filters on July 20 and H images with the H_2 filter on July 23. These sites were well separated from neighbors, and observed continuously from the morning limb until disappearing in the evening limb. The impact times of G, H, and L fragments are 18:07:33 (day:hour:min), 18:19:33, and 19:22:21 in July, according to Hammel et al (1995)'s estimation from Hubble Space Telescope's images. The impact sites were only a few days old, and their shapes suggested no significant change of the dust layers since formed from the impacts.

Reflectances of L and G images taken with the H_2 and CH_4 filters are shown with models in Figures 5 and 6, respectively. The first apparent feature in these figures is that the observed I/F's do not decrease near CML. This implies that the dust layers have optical depth greater than 1, as explained in the previous section. A thin layer has a lower value of reflectance near the CML than near the limb since it is transparent to lights coming in near perpendicular direction to the layer. Significant amounts of impact dusts must be produced in these impacts and floated in the atmosphere at the time of observation.

The reflectances of G and L sites near CML are approximately 0.5 for the H_2 filter, whereas the reflectance of G sites is 0.35, approximately 0.15 than that of L sites for the CH_4 filter. Since CH_4 absorption at 2.3 μm is much stronger than H_2 absorption at 2.12 μm, a small difference between the altitude levels of the two dust layers may have resulted in reflectance difference in the CH_4 images, but not in the H_2 images. Different combinations of ω, τ, and τ_a for the two dust layers could result in about the same reflectance for the H_2 filter as the observation suggests. However, it is unlikely that the characteristics of impact dust particles (e.g. single scattering albedo) are drastically different from one site to another, since the fragments originated from the same comet. It is also unlikely that any

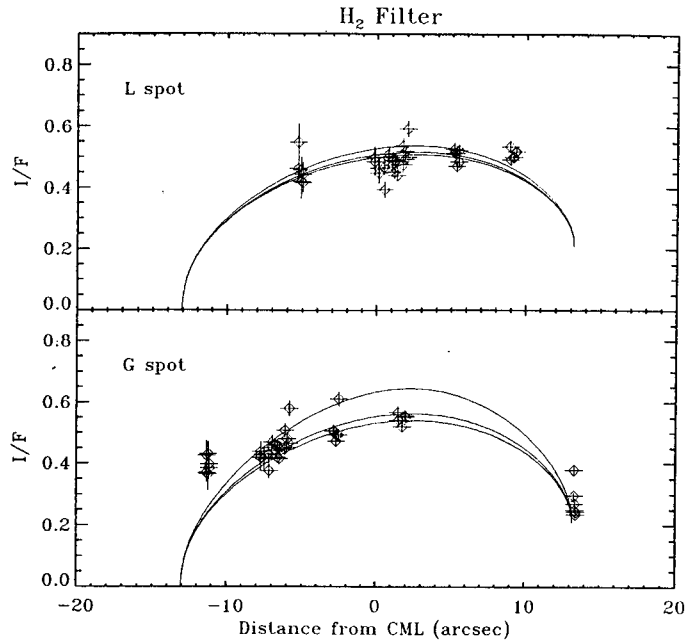

Fig. 5. Comparision of observed and model reflectances of L and G sites taken with the H_2 filters. For the L site, model reflectances were computed with $\omega = 0.999$ and $\tau = 1, 2, 5$ (from lower to upper). For the G site, they were computed with $\omega = 0.999$ and $\tau = 5$, 10, and a limiting case of $\omega = 1$ (from lower to upper).

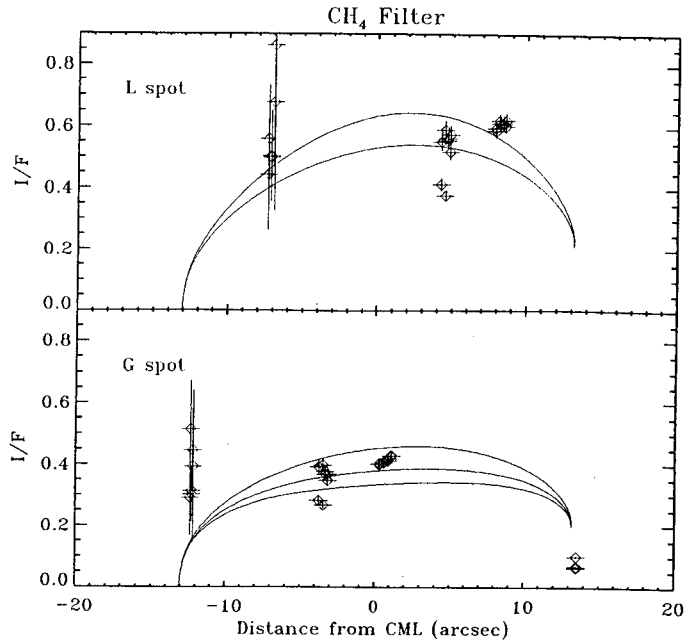

Fig. 6. Comparision of observed and model reflectances of L and G sites taken with the CH_4 filters. For the L site, model reflectances were computed with $\omega = 0.999$ and $\tau = 5$, and a limiting case of $\omega = 1$ (from lower to upper). For the G site, they were computed with $\omega = 0.99$ and $\tau = 1$, 2, and 5 (from lower to upper).

difference in τ_a had been compensated by difference in τ. The reflectance increases insensitively with the optical depth of a dust layer but decreases very sensitively with the optical depth above the dust layer. Therefore, both G and L at the H_2 images seem to have about the same values of ω, τ, and τ_a. Since ω and τ may not change rapidly with wavelength, both sites at the CH_4 images may have similar values of ω and τ, too. Thus, the difference

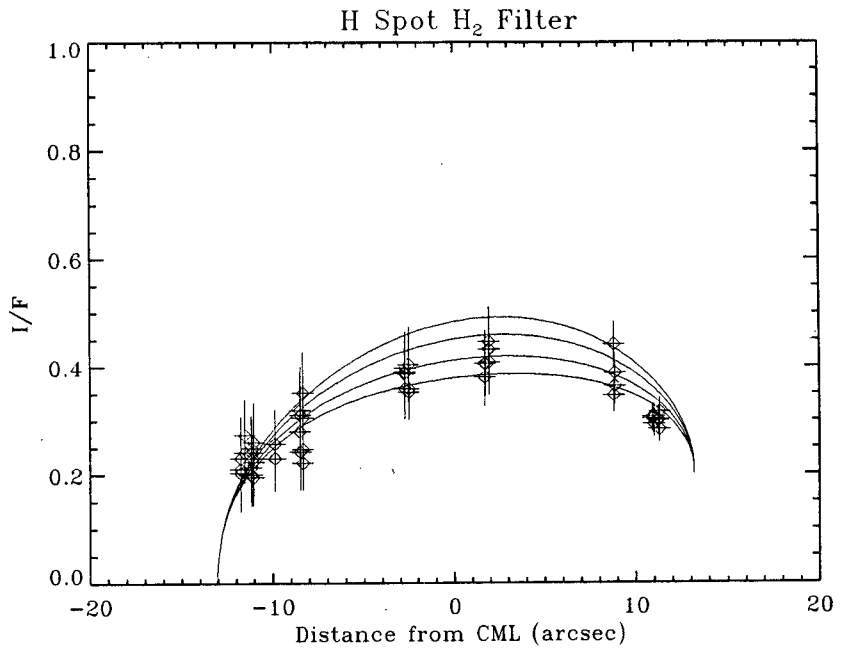

Fig. 7. Comparision of observed and model reflectances of H site taken with the H_2 filter. The model reflectances were computed with $\omega = 0.99$ and $\tau = 2$, 3, 5, and 10 (from lower to upper).

of reflectance between the G and L sites should be due to difference in τ_a's, or altitude levels. In other words, the altitude of the dust layer in G site is a little lower in the Jupiter's atmosphere than that in the L site. This inference is consistent with the fact that G site had more time (38 hours) to settle the dust layer than L site since they were formed from the impacts.

Most of reflectances in figure 5 and 6 are in the range of 0.35 - 0.6, suggesting that the single scattering albedo, ω, is close to 1 and the dust layers are at high altitudes. For the limiting case of $\omega = 1$, the model reflectance is 0.6 at CML for $\tau_a = 0.01$ regardless of the optical depth of a dust layer. In order to fit the observed reflectance range, we find that τ_a should not be significantly greater than 0.01 since the reflectance decreases sensitively with τ_a. We adopt a nominal value of 0.01 for τ_a in the models presented in the Figures 5, 6, and 7. In Figure 5, the low, middle and high curves for the L site were computed with combinations of $(\omega,\tau) = (0.999, 1)$, $(0.999, 2)$, and $(0.999, 5)$, respectively, and the three curves for the G site are for the combinations of (0.999,5), (0.999,10), and a limiting case of $\omega = 1$, respectively. In Figure 6, the lower and upper curves for the L site are for the combination of (0.999, 5) and the limiting case, respectively and the lower, middle, and upper curves for the G site are for the combinations of (0.99,1), (0.99,2), and (0.99,5), respectively. The observed reflectances seem overall consistent with models for $\omega \geq 0.99$ and $\tau \geq 2$, although the observed reflectances near the limb show significant deviations from the models. The apparent area of an impact site becomes smaller as it approaches to the limb, which makes difficult to estimate an intensity of the site due to atmospheric seeing effects.

Figure 7 shows reflectances of H site on July 23 with model reflectance curves of $\tau = 2$, 3, 5, and 10 (from lower to upper) for $\omega = 0.99$. The models with $\tau = 2$ - 5 fit well with observations in all locations. These parameters for the H site are very similar to those inferred from the G and L sites as discussed previously, despite that the H impact site was observed to be significantly smaller than the G and L sites. The impact dust layers, therefore, seem to be formed from similar processes independent of the magnitude of impact explosion. Observations with the HST have noted that the SL9 impact explosion fireballs reached at about the same altitude above the limb of Jupiter for all observed fragments (Hammel et al, 1995). And then re-entry shocks of the falling fireballs may heat the atmosphere again and form dust layers at the same altitude regardless of the magnitude of the explosions. A stronger explosion may result in a larger amount of dusts, but in the same single scattering albedo, thickness and altitude of a dust layer as for a weaker one.

V. CONCLUSIONS

We have obtained near-infrared images of Jupiter impacted by comet Shoemaker-Levy 9 on Jupiter before during and after the impacts. The impact sites are clearly seen in images taken with the CH_4 (2.3 μm) and H_2 (2.12 μm) filters, and are marginally visible in images with the K band (2.0 μm) and NH_3 (1.50 μm) filters. An impact site consists of a dust layer that reflects sunlight efficiently. Comparisons of reflectances of G, L, and H sites with simple radiative transfer models suggest that optically thick dust layers were formed. The comparisons also suggest a very small optical depth (on the order of 0.01) due to absorption by H_2 or CH_4 molecules, indicating that the dust layers were at high altitude. The dust layers in these sites seem to form at about the same altitude regardless of the magnitude of the impacts, but they appear to descend gradually after the impact. The dust layers have optical depths of 2 - 5, according to the models. Effective albedo of the dust layers do nat vary significantly in the wavelength range of 1.5 - 2.3 μm, and about the same as for ammonia cloud tops at 1.58 μm. The albedos of the dust layers seem to be very different from that of polar haze.

ACKNOWLEDGEMENT

This work is supported by the grant from the Korea Astronomy Observatory.

REFERENCES

Chamberlain, J.W. and D.M. Hunten 1987, *Theory of Planetary Atmospheres*, pp 163, Academic Press, 2nd ed., San Diego.
Chandrasekhar, S. 1960, *Radiative Transfer*, Dover, New York.
Clark, R.N. and T.B. McCord 1980, *Icarus*, **43**, 161.
Hammel, H.B. et al. 1995, *Science*, **267**, 1288.
Kim, S.J. et al. 1991, *Icarus*, **91**, 145.
Kim, Y.H. and S.J. Kim, 1996, *submitted to Journ. Aston. Space Sci.*
Nash, D.B. et al. 1986, *Satellites*, pp 636-637, eds. J.A. Burns and M.S. Mathews, Arizona Press.
Orton, G. et al, 1995, *Science*, **267**, 1277.
Sekanina, Z. 1994, *submitted to Science*
Weaver, H.A. et al. 1995, *Science*, **267**, 1282.
West, R.A. et al. 1995, *Science*, **267**, 1296.
Zahnle, K. and M.-M. MacLow 1994, *Icarus*, **108**, 1.